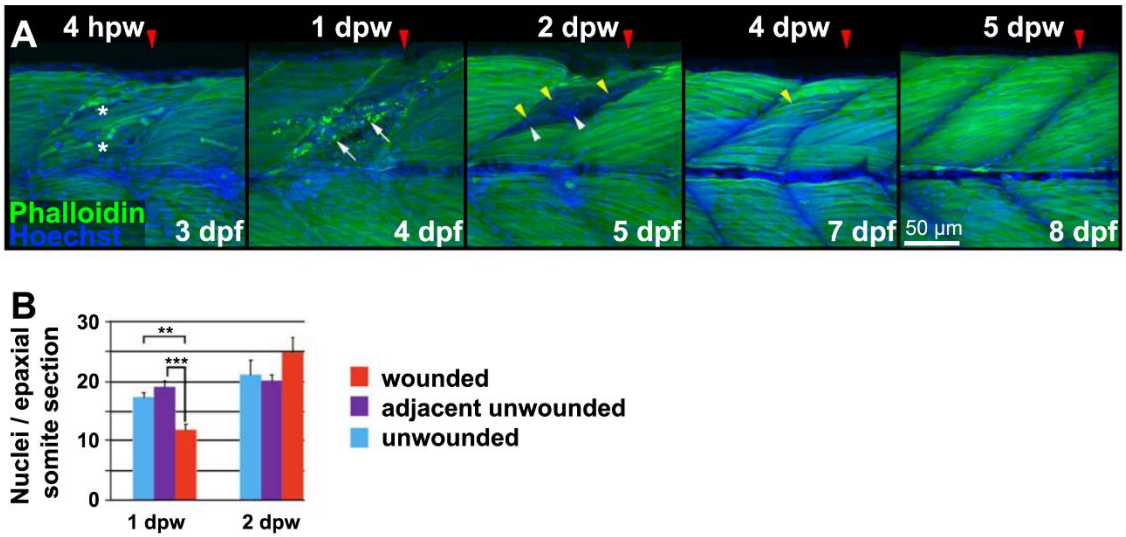

Supplementary Figure S1. Cellular changes in wounded muscle.

A. Lateral confocal image stack projections of wounded epaxial somites (red arrowhead) in larvae wounded at 3 dpf and analysed 4 hours post wounding (hpw) or 1-5 dpw. Fixed larvae were stained for F-actin (Phalloidin) and nuclei (Hoechst). Note the broken fibres (asterisks) and rounded nuclei at the 4 hpw wound site. Loss of regular striation and presence of actin aggregates at 1 dpw (arrows) is followed by accumulation of nuclei in the wound site at 2 dpw (arrowheads). At 2 dpw, striations begin to reappear in thin fibres (yellow arrowheads) at the wound edge, and are abundant by 4 dpw. Dorsal to top, anterior to left. Bar = 50 µm.

B. Quantification of nuclei per confocal transverse cross-section of epaxial somites that were wounded (red), adjacent to wound but unwounded (purple) and in unwounded fish (blue). Half the nuclei at the horizontal myoseptum were attributed to the epaxial somite.

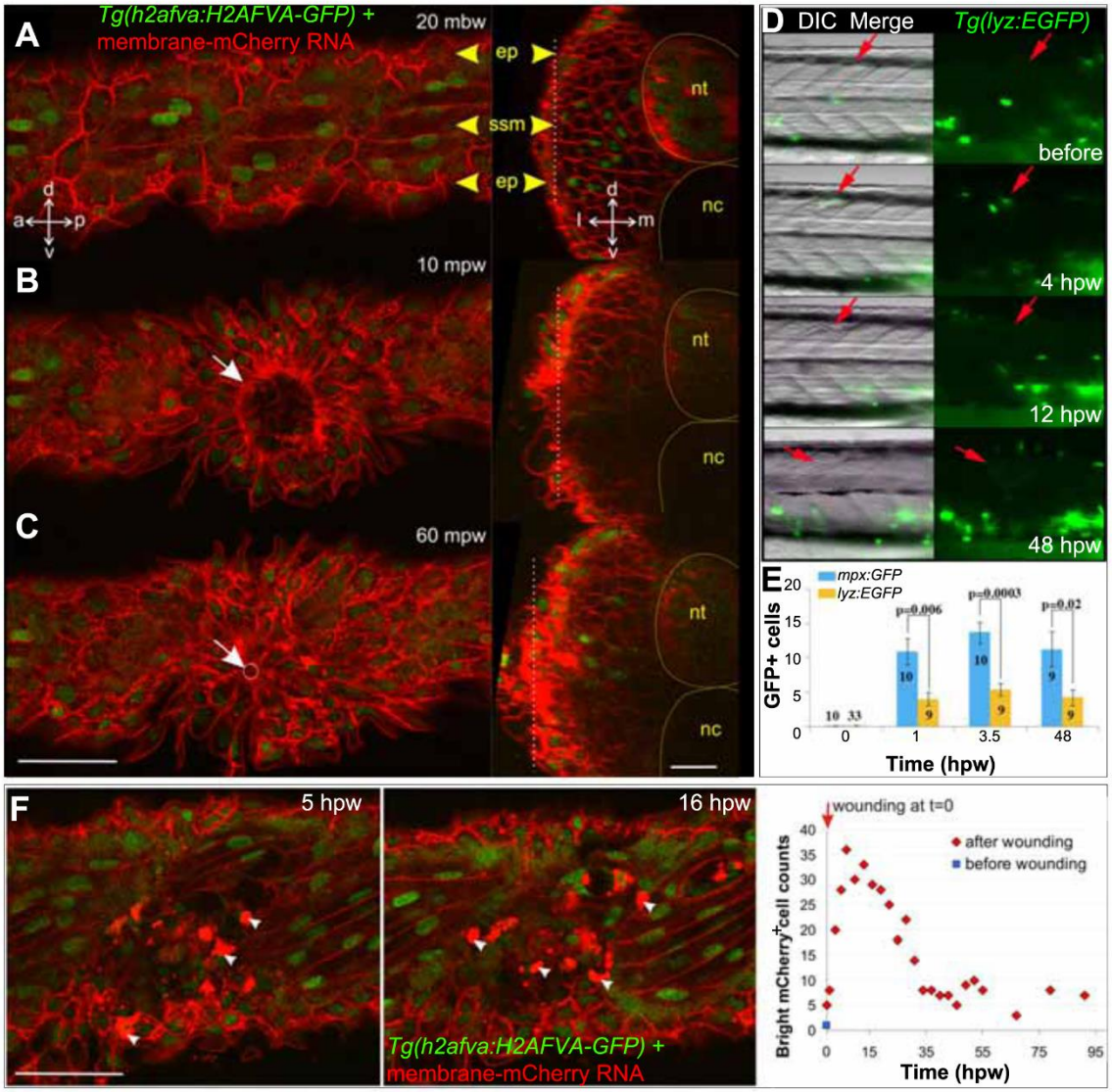

Supplementary Figure S2. Epidermal and leukocyte movements during wound closure. **A-C.** Rapid epidermal wound closure in a 2.5 dpf membrane-mCherry RNA-injected *Tg(h2afva:H2AFVA-GFP)* larva in optical parasagittal section (left), taken at the level of the white dotted line in the transverse sections (right). **A.** Before wounding, polygonal epidermal cells (ep) overlie superficial slow muscle cells (ssm). **B.** At 10 mpw, an epidermal ring already formed (white arrow) and was almost closed at 60 mpw (**C**, white circle and arrow). Transverse sections show that the epidermal region above the wound thickens by some 10–15 µm.
D. *Tg(lyz:EGFP)* fish were wounded around s12 at 2.5 dpf (red arrows) and imaged in lateral view with dorsal up and anterior to left. GFP+ cells accumulated at wound site 4 hpw.
E. *Tg(mpx:GFP)* and *Tg(lyz:EGFP)* were wounded in two to four somites between epaxial s5-12 at 2.5 dpf. GFP+ cells were counted at the wound site of the number of fish indicated.
F. Change in number of bright mCherry cells (arrowheads) with time in membrane-mCherry RNA-injected *Tg(h2afva:H2AFVA-GFP)* larva wounded at 2.5 dpf. a - anterior, d - dorsal, l - lateral, m - medial, nc - notochord, nt - neural tube, p - posterior, v – ventral. Bars = 50 µm.

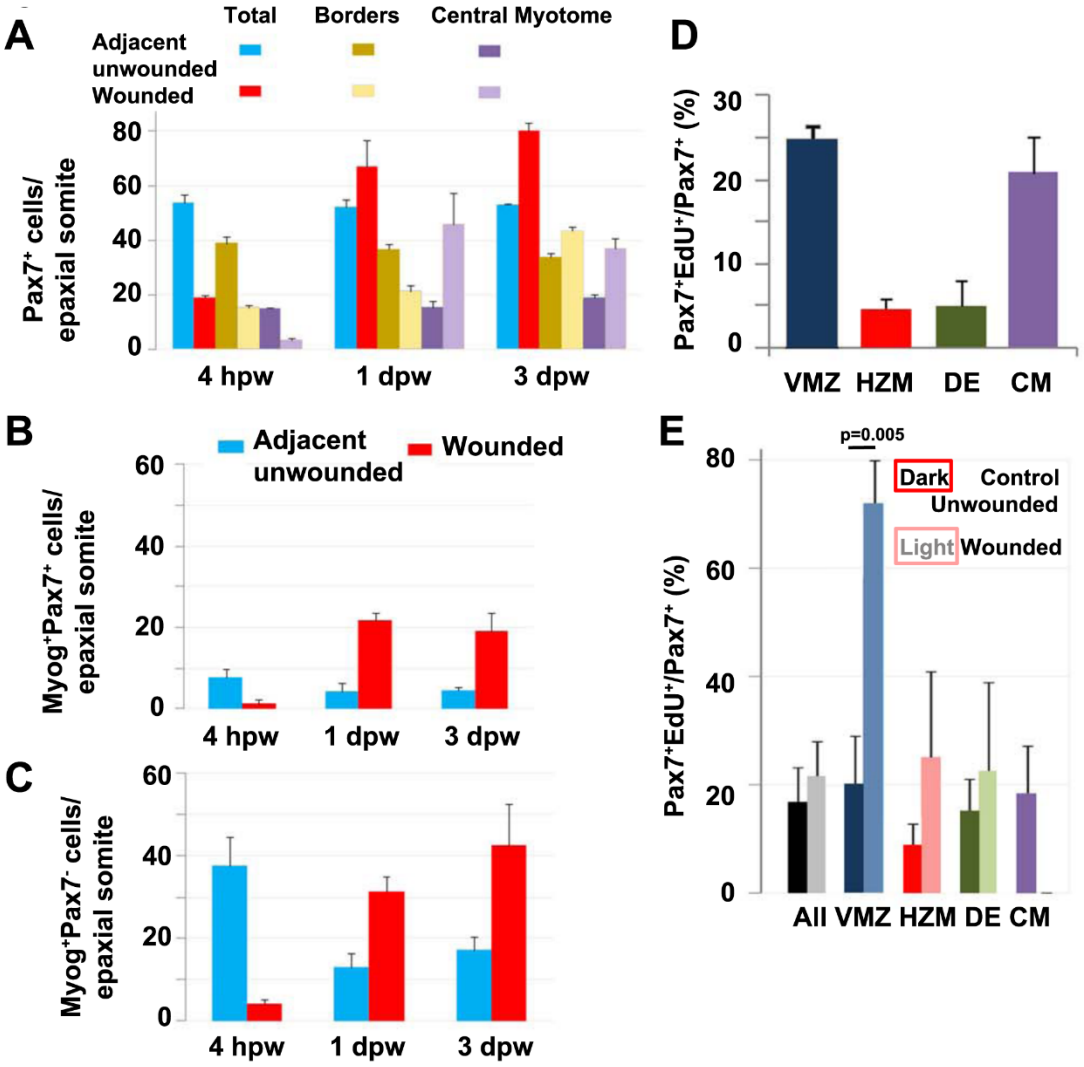

Supplementary Figure S3. Pax7, Myog and S-phase cells increase in wounded muscle. Wholemount wild type larvae at 3 dpf with large mechanical wounds were fixed at 4 hpw, 1 dpw or 3 dpw and immunostained for Pax7 and Myogenin. Cell counts show total mononucleate $Pax7^+$ by somitic region in wounded (red) and unwounded (blue) somites (A) or $Myog^+Pax7^+$ (B) and $Myog^+Pax7^-$ cells (C) in epaxial somites of four larvae at each time-point. **A:** At 4 hpw, the total number of Pax7+ cells was reduced ($p=1.71 \times 10^{-5}$). $Pax7^+$ cells located within one nuclear length of vertical or horizontal myoseptum or dorsal somite edge ('Borders', p=0.003) or in remainder of somite ('Central Myotome', $p=5.24 \times 10^{-5}$) were reduced compared to adjacent unwounded somites. By 1 dpw, the number of $Pax7^+$ cells in total (p=0.03), at borders (p=0.0006) and in central myotome (p=0.03) was increased compared to the respective $Pax7^+$ levels at 4 hpw in wounded epaxial somites. Moreover, the total number of $Pax7^+$ cells was similar between adjacent unwounded and wounded epaxial somites at 1 dpw, although elevated in wounded central myotome (p=0.04) and reduced at the borders (p=0.002) when compared to adjacent unwounded epaxial somites. The number of $Pax7^+$ cells at 3 dpw was increased in wounded epaxial somites: total (p=0.01), at borders (p=0.007), and in central myotome (p=0.01) compared to adjacent unwounded epaxial somites. **B:** $Myog^+Pax7^+$ cells in central myotome of wounded somites were reduced at 4 hpw (p=0.02), increased at 1 dpw (p=0.0006) and similar at 3 dpw (p=0.05) compared to adjacent unwounded epaxial somites. **C:** The number of $Myog^+Pax7^-$ cells in the central myotome of wounded somites were reduced at 4 hpw (p=0.017), increased at 1 dpw (p=0.009) and similar at 3 dpw (p=0.05) compared to adjacent unwounded epaxial somites. **D,E.** Fraction of 3 h EdU-marked $Pax7^+$ somite cells by region in unwounded somites 16-18 of three 4 dpf (D) or at 5 hpw in five wounded and three control 3 dpf larvae (E). VMZ vertical myoseptum, HMZ horizontal myoseptum, DE dorsal edge, CM central myotome. Error bars are s.e.m.

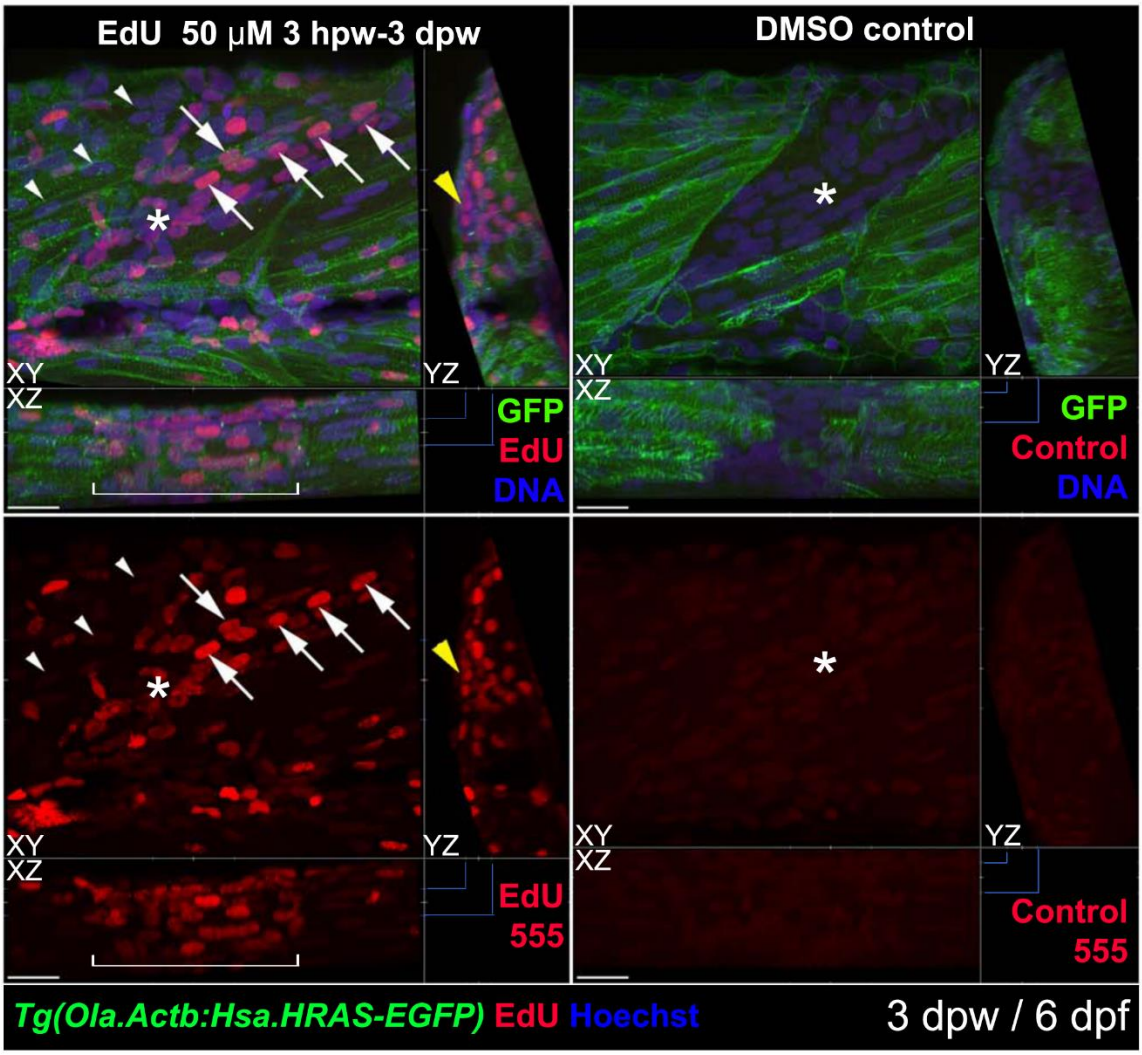

Supplementary Figure S4. Most nuclei in wound sites have undergone S-phase. *Tg(Ola.Actb:Hsa.HRAS-EGFP)* larvae were wounded at 3 dpf in epaxial somite S17 and treated with EdU (left) or control vehicle (right) from 4 hpw until 3 dpw/6 dpf, followed by immunodetection of anti-GFP-Alexa488, ClickIT-555 for EdU and Hoechst for DNA. 3D confocal stacks were processed with Imaris to make short orthogonal projections from the planes indicated by the blue markings. The wounded somite region (white bracket) contains abundant nuclei, most of which are EdU-marked. Many nuclei have the typical elongated form and alignment of fibre nuclei (arrows). Other regions of the wound still contain nuclei with rounded morphology (asterisks). The transgene membrane GFP labels some regenerating cells weakly (right), for reasons that are unclear. Adjacent unwounded somites contain numerous nuclei unmarked by EdU (arrowheads) and some EdU-marked nuclei, possibly reflecting normal growth. Note the abundant EdU label in superficial cells reminiscent of dermomyotome (yellow arrowhead). 16/20 EdU-treated individuals showed all these features. Bars = 20 µm.

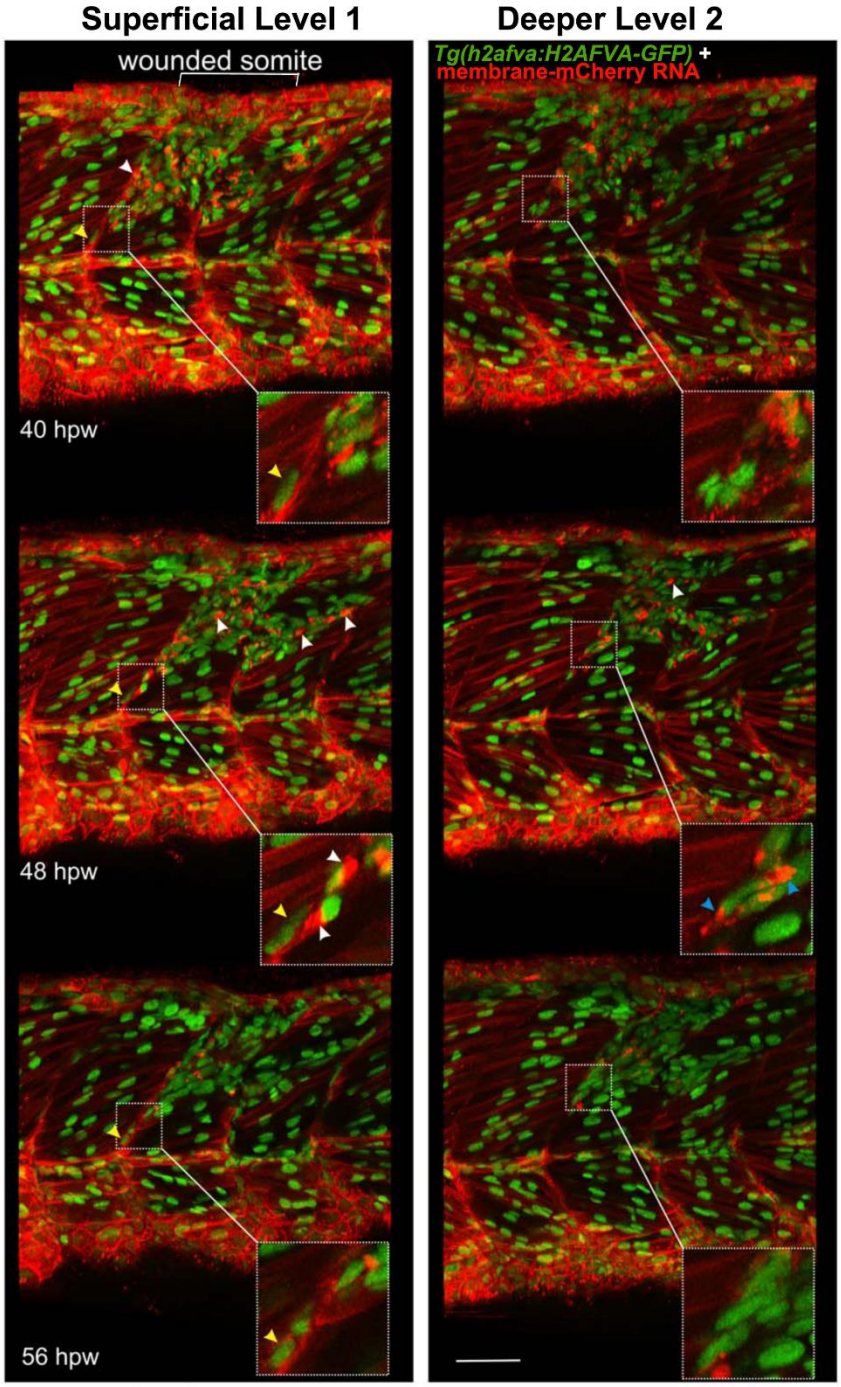

Supplementary Figure S5. Cells with specialised morphology at borders of wounded somites.
Time-lapse of short stacks of lateral confocal sections from larva in Movie S1, anterior to left. Wounded region is indicated (white bracket). Level 1 is about 30 μm more superficial than Level 2 revealing the extent of damage. Boxed insets show vertical myoseptal (VMZ) region. Some cells aligned with the VMZ (yellow arrowheads) move little between time-points. Other cells aligned at the VMZ had a small oval nucleus and a bright 'cap' of membrane mCherry (white arrowheads) and appeared at the lesion site between 32-40 hpw, but could not be identified at the VMZ at subsequent time-points, suggesting rapid migration or change of appearance. At 48 hpw, such 'capped' cells were dispersed in the central myotome and more numerous, but their number subsequently declined. Some cells at the VMZ appeared to have unusually elongated nuclei and bright bipolar cytoplasmic mCherry, suggesting that they might be dividing cells (blue arrowheads). The labelling of all cells and the low time resolution of the movie prevented observation of such events as MPC proliferation and fusion in real time. Bar = 50 μm.

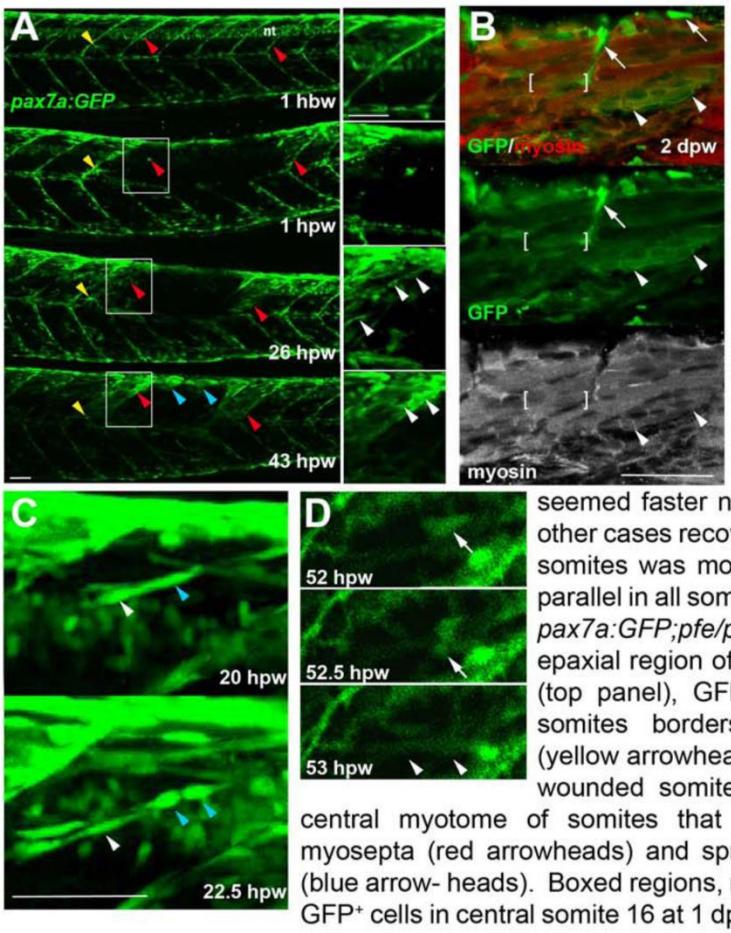

Supplementary Figure S6. Genetically marked p*ax7a*-expressing cells contribute to regeneration. *Pax7a:GFP* zebrafish larvae wounded at 3-4 dpf were repeatedly confocally scanned live embedded in agarose (A,C,D) or fixed and stained (B). All larvae are shown in lateral view, anterior to left, dorsal up. Repair of large wounds followed a variable spatiotemporal course, likely reflecting variability in the extent of initial wounding. Whereas in some cases repair seemed faster near to unwounded somites (A), in other cases recovery at the dorsal edge of wounded somites was more rapid and repair progressed in parallel in all somites (see Fig. S7). **A**. Time lapse of *pax7a:GFP;pfe/pfe* larva wounded at 4 dpf in the epaxial region of somites 16-20. Prior to wounding (top panel), GFP is present in neural tube (nt), somites borders and a residual xanthophore (yellow arrowheads), which marks the anteriormost wounded somite. Note the recovery of GFP in central myotome of somites that retained GFP^{+} cells at vertical myosepta (red arrowheads) and spreading from dorsal epaxial edge (blue arrow- heads). Boxed regions, magnified at right, show elongating GFP^{+} cells in central somite 16 at 1 dpw (white arrowheads) yielding thin muscle fibres by 2 dpw. In large wounds, most pax7a:GFP signal was lost at the wound site, consistent with ablation of many muscle precursor cells. By 1 dpw, pax7a:GFP+ cells began to re-accumulate from the edge of the wounded region, occupying the centre of wounded somites and seeming to elongate (insets). At 2 dpw, pax7a:GFP-expressing cells contributed to muscle fibre regeneration, as demonstrated by the appearance of GFP in elongated multinucleate muscle fibres containing myosin heavy chain (compare A with B).
B. Immunodetection of pax7a:GFP and myosin heavy chain (MyHC) two days after wounding two adjacent somites revealed mononucleate GFP^{strong}MyHC^{-} cells (arrows), thin GFP^{medium}MyHC^{weak} nascent fibres with unstructured MyHC (arrowheads) and larger GFP^{weak}MyHC^{+} maturing fibres with recognisable sarcomeric structure (between brackets). The pax7a:GFP signal rapidly weakened as fibres enlarged, often requiring immunodetection to reveal the GFP in maturing regenerated fibres. Strikingly though, the number of pax7a:GFP-labelled cells in somites in the central region of large wounds remained low; most labelled mononucleate cells were present in somites at the wound edge, where new GFP-labelled fibres also first appeared (see A 43 hpw). It therefore appears that *pax7a:GFP* marked cells at wound edges initially contributed to muscle regeneration.
C. Brief time lapse series of short stacks showing pax7a:GFP^{+} cells dividing (blue arrowhead) and migrating (white arrowhead). Such detailed time-lapse analysis confirmed that *pax7a:GFP* marked cells migrate and divide, consistent with their re-accumulation in the lesion.
D. Brief time-lapse series of single plane showing pax7a:GFP^{+} cell moving (arrows) and then fusing into a fibre (arrowheads). After entering the wound a proportion of cells fuse into nascent fibres. These results show that Pax7a^{+} cells at the dorsal and vertical somite border can initiate fibre regeneration. Bars = 50 μm.

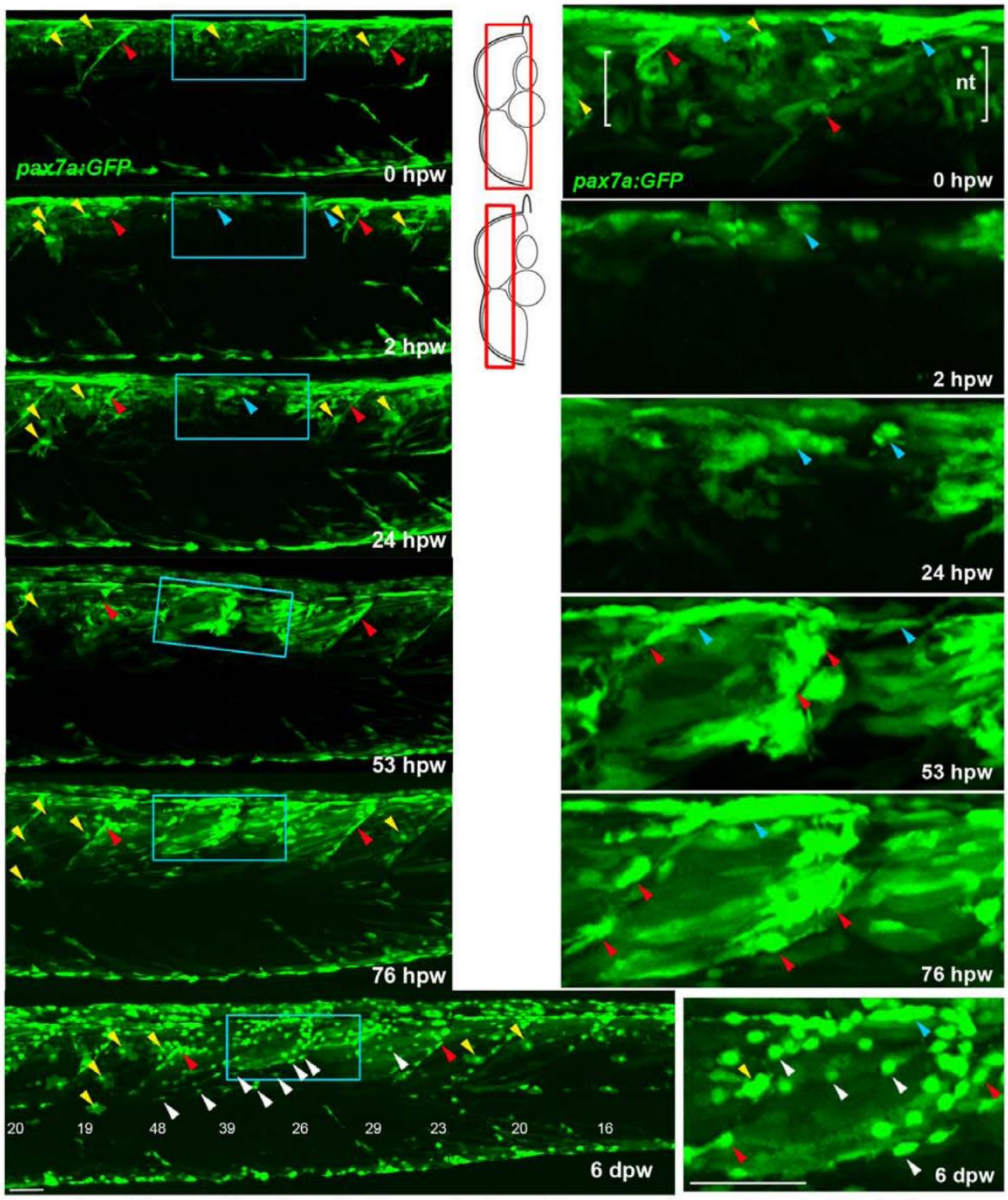

Supplementary Figure S7. Genetically marked *pax7a*-expressing cells contribute to regeneration. *Tg(pax7a:GFP);pfe/pfe* zebrafish larva was wounded at 4 dpf in the epaxial region of somites 16-19 and repeatedly confocally scanned live, embedded in agarose. Maximum intensity projections of selected regions of the stack are shown in lateral view, anterior to left, dorsal up. Only top panel includes neural tube levels (red boxes in schematics). Blue boxed regions, magnified at right, show GFP$^+$ cells near dorsal epaxial edge in central somite 16 at 1 dpw yielding thin muscle fibres by 2 dpw (blue arrowheads). Prior to wounding (top panels), GFP is present in cells of neural tube (nt, between brackets), dorsal and vertical somite borders (blue and red arrowheads, respectively) and rare xanthophores (yellow arrowhead). In contrast to the larva in panel S6A, GFP recovers more rapidly in central wounded somites (blue box) that had GFP$^+$ cells spreading from dorsal epaxial edge at 24 hpw (blue arrowheads). pax7a:GFP$^+$ cells began to re-accumulate at the dorsal edge by 1 dpw and fibre formation was well underway by 2 dpw. As nascent fibres matured and increased in volume, their GFP fluorescent intensity declined, while small myogenic cells remained strongly labelled. In contrast to the larva in panel S6A, GFP recovers more rapidly in central wounded somites (blue box) that had GFP$^+$ cells spreading from dorsal epaxial edge at 24 hpw (blue arrowheads). At 6 dpw, when wound repair was advanced, numerous small round GFP$^+$ cells (white arrowheads) appear in all somites overlying the myotome, in the dermomyotome location. These cells were more numerous in wounded somites than in adjacent unwounded somites, and concentrated at the posterior somite border. In summary, *pax7*a-expressing myogenic cells contribute to muscle repair and a sub-population of such cells remains undifferentiated after myotome recovery. Bar = 50 μm.

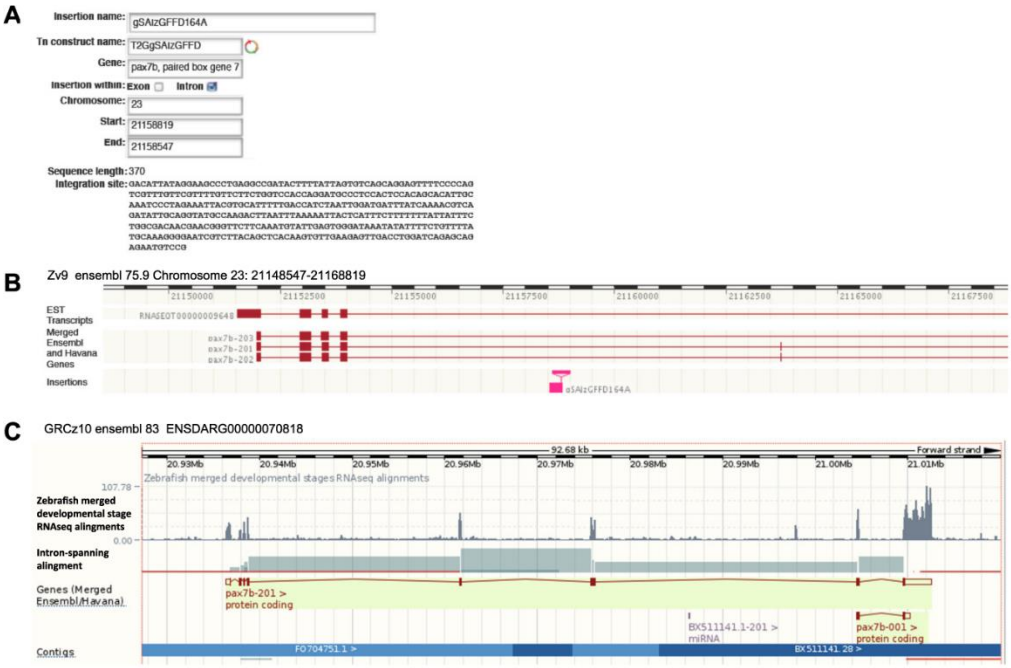

Supplementary Figure S8. Integration site of gSAIzGFFD164A in *pax7b*.

A. Tol2-mediated integration site was determined by inverse PCR from the integrated vector sequence in the zTrap screen.

B. Integration site mapped by BLAST to the fourth intron of *pax7b* on chromosome 23 (based on Ensembl Zv9) 4.8 kb 3' of exon 4. Note the presence of a short 5th exon 9.7 kb 3' of exon 4 that is lacking in GRCz10.

C. Ensembl GRCz10 version 83 (December 2015) showing the *pax7b* gene with a large 22.5 kb 4th intron and lacking RNAseq evidence for alternative-splicing of a short 5th exon.

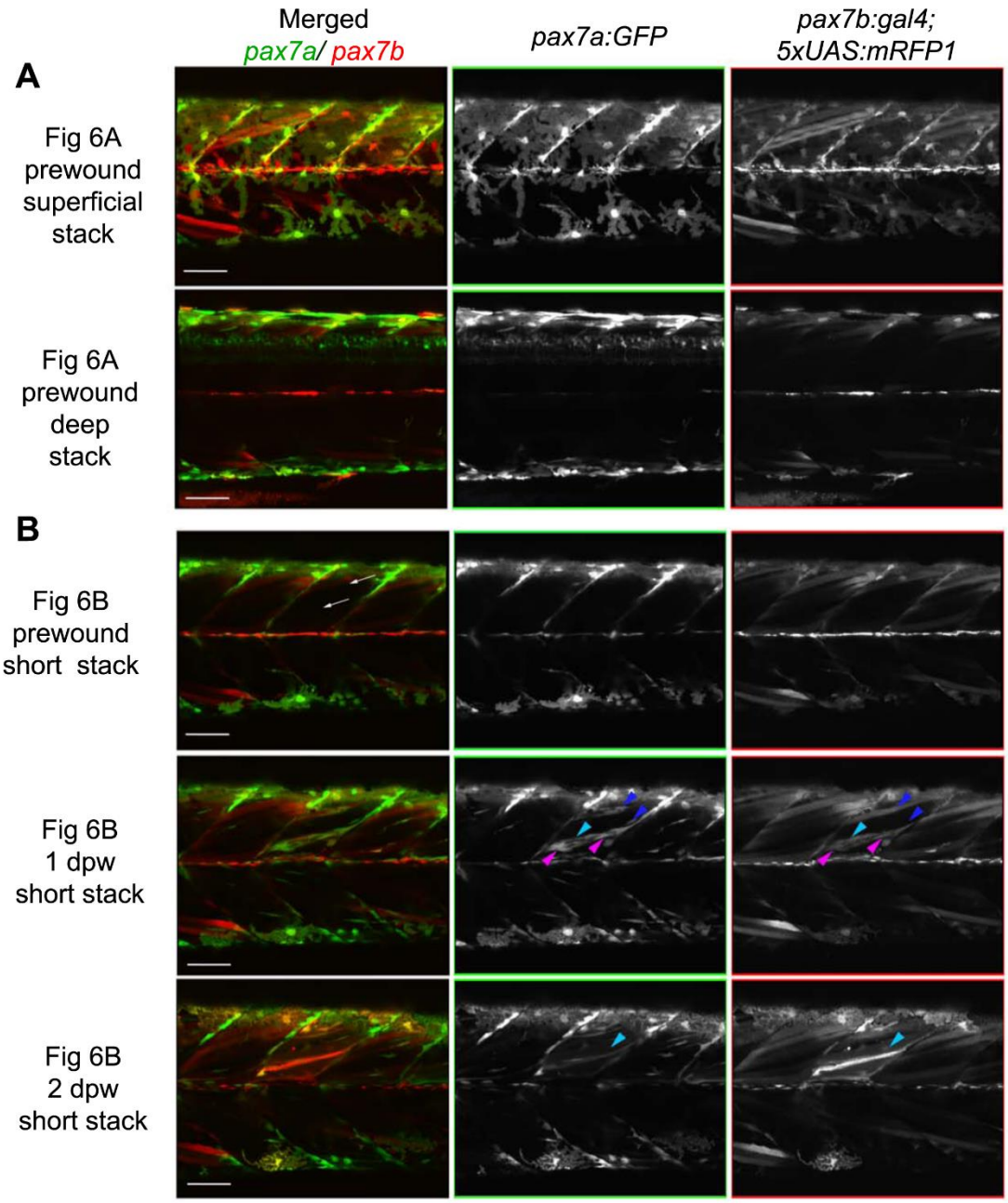

Supplementary Figure S9. Individual green and red channels showing fusion of pax7a- and pax7b-reporter cells during wound repair (from Fig. 6A,B). Lateral confocal maximum intensity projection stacks of pre-wound (upper three rows, from Fig. 5A) and post-wound (lower two rows, from Fig. 5B) yolk extension somites of a *pax7a:GFP;pax7b:RFP* larva, anterior to left, dorsal to top. **A.** At 3 dpf, prior to wounding, xanthophores have strong GFP and weak RFP, neural tube cells have strong GFP and little RFP, whereas superficial muscle fibres have RFP but lack GFP. **B.** Short stack of epaxial wounded somite region excluding deep and superficial regions. Prior to wounding, no *pax7a:GFP* cells and only a *pax7b:RFP* large fibre are present in the deep somite. Two oblique needle insertions made two small lesions in a single epaxial somite (white arrows). By 1 dpw, rare *pax7a:GFP*-only cells (blue arrowheads) and abundant dual-labelled cells (magenta arrowheads) elongate in wound. Rare weak *pax7b:RFP* cells with little or no GFP (cyan arrowheads) are also present. By 2 dpw, time-lapse reveals several nascent fibres marked strongly by RFP and weakly by GFP. Rounded *pax7b:RFP* cells are still present in the wound regions, but *pax7a:GFP*-only cells are diminished. Bars = 50 μm

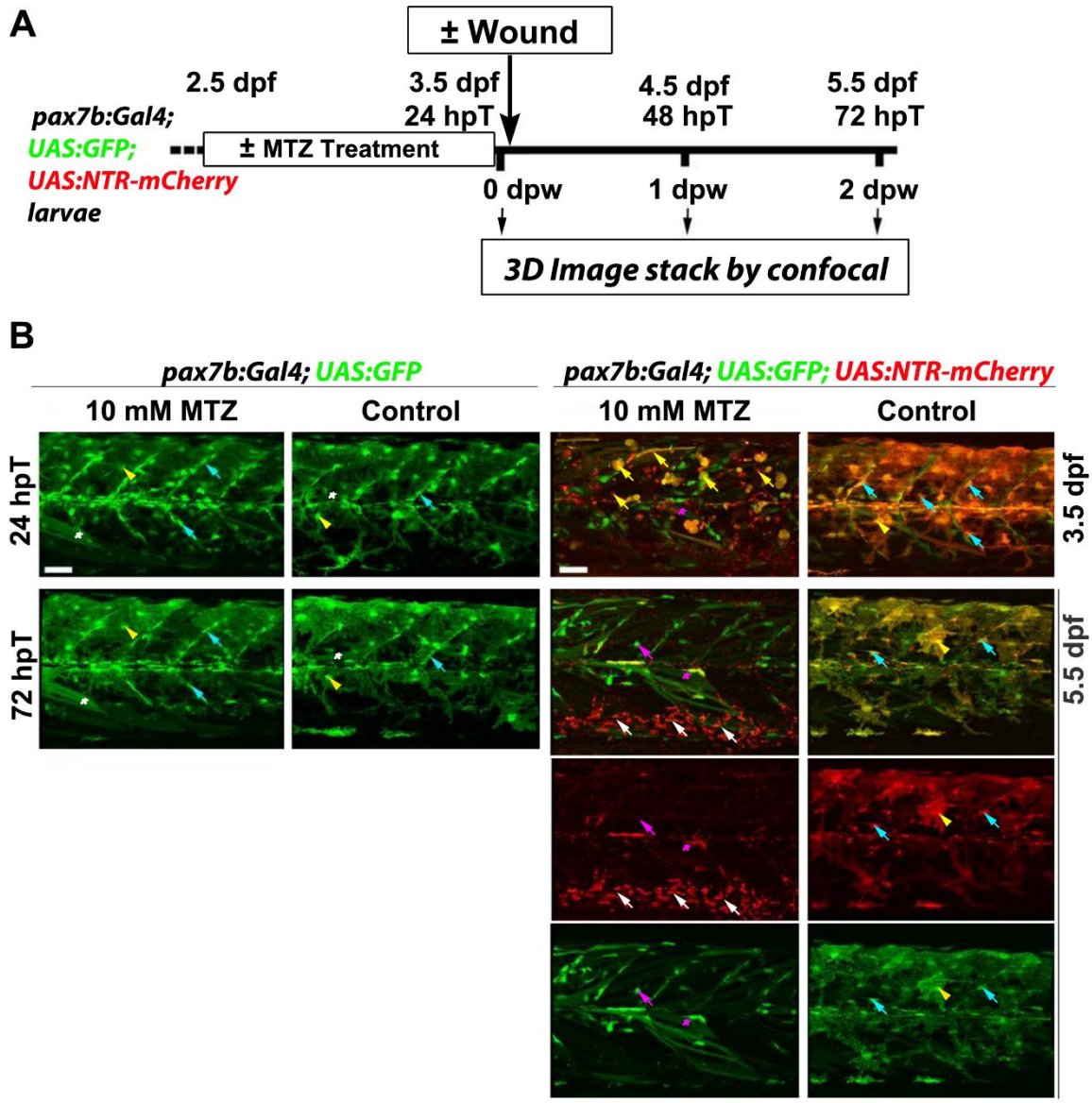

Supplementary Figure S10. MTZ specifically ablates *pax7b:NTR-mCherry* cells.
A. Work flow of metronidazole (MTZ) mediated selective ablation of cells expressing nitroreductase (NTR) from *pax7b*-driven NTR-mCherry cells (hpT, hours post start of MTZ treatment; dpw, days post wound; dpf, days post fertilisation).
B. Larve of the indicated genotype were treated with 10 mM MTZ or DMSO vehicle/control from 2.5 dpf to 3.5 dpf and not wounded. Lateral maximum intensity projection of stacks from the same (except righthand column) 24 hpT/3.5 dpf and 72 hpT/5.5 dpf embryos are shown. Bottom two rows show single channels of 5.5 dpf merge above. Controls lacking NTR (two lefthand columns) show that MTZ is not toxic without NTR. Marked fibres (white asterisks), xanthophores (yellow arrowheads) and MPCs (cyan arrowheads) survive treatment. In control DMSO-treated dual-labelled fish, GFP and mCherry largely overlap at 3.5 dpf in MPCs and xanthophores (right column). MTZ treatment of NTR-expressing larvae eliminated most of the mCherry MPCs and xanthophores, leaving dying cells (yellow arrows) that were eliminated by 72 hpT. Low numbers of GFP-only cells and fibres remained (magenta arrow and asterisks). By 3 days after MTZ treatment, almost all mCherry debris had been cleared and numerous motile phagocytes were present ventrally around major blood vessels (white arrows; GFP had been lost immediately upon engulfment). GFP shows reduction of *pax7b*-expressing cells. No re-appearance of mCherry was observed in MPCs or other cells. Bars =50 μm.

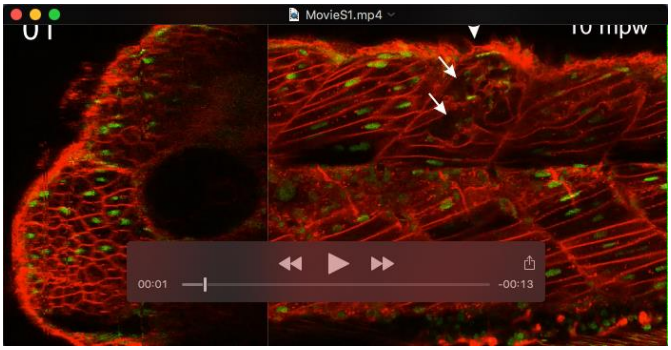

Movie 1. *In vivo* imaging of larval zebrafish muscle regeneration.

Transgenic larvae from the ubiquitous *Tg(h2afva:H2AFVA-GFP)*^{kca66} line injected with membrane mCherry RNA were wounded in somite 17 at 3.5 dpf and imaged by 3D confocal time-lapse microscopy for 200 hpw (8.5 dpw) at 8 hour intervals, n = 5 larvae. Movie shows the same region of the injured somite of one larva in transverse (left) and parasagittal (right) views abstracted from 3D stacks at each imaged time point (number in top right). Dorsal to top and lateral (la) or anterior to left, respectively. Extensive cavities form in the wound between 8–32 hpw (white arrows). From 32 hpw, small round nuclei are localized to the lesion (yellow arrows) but by 8 dpw the nuclei at the lesion have taken on an elongated cigar-shaped appearance (pink arrowheads). Photobleaching due to imaging is evident in nuclei and fibres of undamaged tissue. Note, however, that mCherry is less bleached in muscle fibres not entirely within the scan field, showing that unbleached membrane mCherry can diffuse into bleached regions along the fibre length. The gradual bleaching of the imaged somites was partially compensated by manually increasing laser power and gain between time points. The whole image was non-linearly enhanced and brightness corrected to compensate for bleaching and facilitate tracking of individual cells, as described in Materials and Methods. Abbreviations: da dorsal aorta; do dorsal; ep epidermis; hms horizontal myoseptum; mbw minutes before wounding; mpw minutes post wounding; nc notochord; nt neural tube; sas parasagittal section; sb vertical myoseptum/somite border; ts transverse section; v ventral; vv ventral vein.

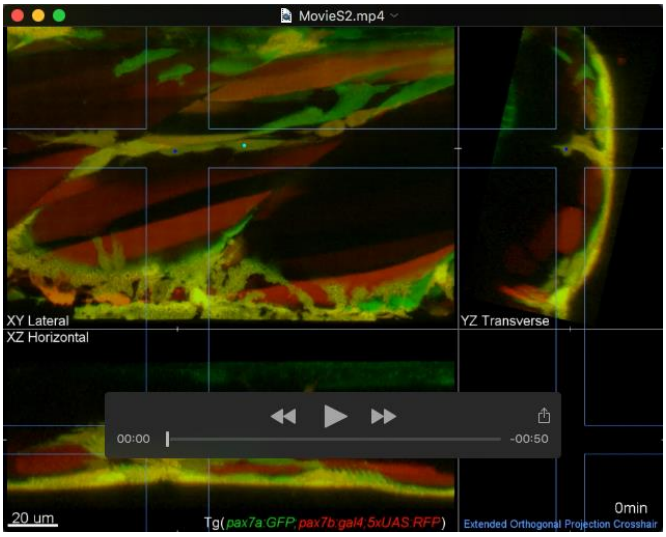

Movie 2. *In vivo* imaging of MPC fusion to pre-existing muscle fibres in larval zebrafish muscle wounds.

Live MPC fusion into pre-existing fibres in epaxial somite wound in a *Tg(pax7a:GFP;pax7b:gal4;UAS:RFP)* 4 dpf larva injured at 3 dpf and imaged at 10 min intervals from 24–40.5 hpw. Four individual *pax7a:GFP;pax7b:RFP* dual-labelled orange MPCs fusing to either unlabelled pre-existing fibres (blue and cyan dots) or RFP^{+} fibres (magenta and yellow dots). The blue MPC contains red puncta and fuses at 90-100min to a deep unlabelled fibre. GFP and some RFP diffuse into fibre cytoplasm leaving red puncta proud of the fibre surface, which subsequently integrate (100-150min; clearly seen in XZ projection). Cyan MPC shows similar behaviour, with dynamic protrusions (200-300min) prior to fusing to a dorsal pre-existing fibre (480-510min; best seen in YZ projection). After a widening of stack depth and change of Z plane (510-530min; indicated by blue crosshairs) the dynamic magenta and yellow cells fuse simultaneously to the same orange fibre (930-940min). XY parasagittal-, XZ horizontal- and YZ transversal maximum intensity extended orthogonal projection views (indicated by blue lines). Magnified snapshot images in merge and red channel at times of fusion are also shown for the blue (Fig. 6A) and magenta and yellow (Fig. 6B) cells. The whole image was non-linearly enhanced and brightness corrected to compensate for bleaching and facilitate tracking of individual cells, as described in Materials and Methods.

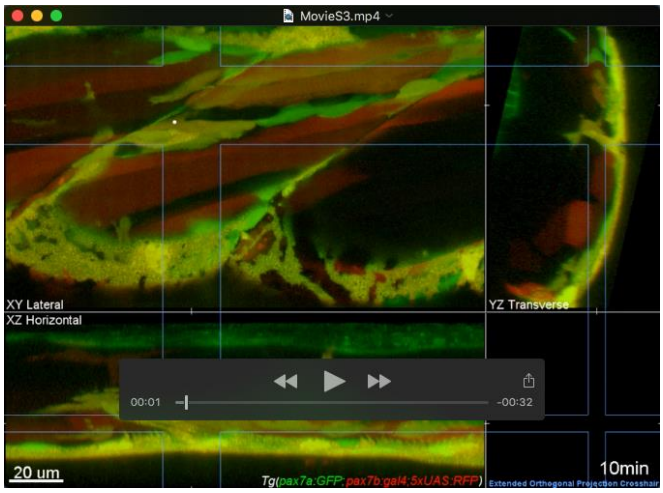

Movie 3 *In vivo* imaging of MPC migration, division and fusion to nascent muscle fibre in larval zebrafish muscle wound.

Live MPC fusion to a nascent fibre in an epaxial somite wound in a *Tg(pax7a:GFP;pax7b:gal4;UAS:RFP)* 4 dpf larva injured at 3 dpf and imaged with 10 min intervals from 24–35 hpw. Two dynamic *pax7a:GFP*-labelled MPCs in the central myotome between two pre-existing large RFP^+ fibres at 1 dpw change position (0-260min) and then elongate to form a thin nascent GFP^+ fibre (260-410min). Simultaneously, a *pax7a:GFP;pax7b:RFP* dual-labelled orange MPC (white dot) aligned with the anterior somite border migrates into the myotome (150-220min), divides (330-370min) and one daughter (white dot) migrates 70 μm along the nascent fibre in 100 min, passing a second dual-labelled MPC and spreading on the surface of an orange fibre (500min). The orange MPC then fuses to the nascent green fibre (510min) as shown by GFP filling the MPC cytoplasm as it retracts processes. Simultaneously, RFP increases in the nascent fibre (best seen in YZ projection) before complete integration (520min). The nascent myotube (still green, but now with a more orange tone) subsequently shows dynamic cytoplasmic and nuclear changes but retains contact with both somite borders until the end of the scan. Snapshot images spanning the time of fusion are also shown in Fig. 6C. The whole image was non-linearly enhanced and brightness corrected to compensate for bleaching and facilitate tracking of individual cells, as described in Materials and Methods.

Table S1. Numerical Raw data and statistical analyses underpinning Figure 7B,C.

Analyses for Fig. 7B on data in first sheet were performed by Two Way ANOVA using Statplus. Output is shown colour-coded sheets. Data for Fig. 7C and analysis are shown on second sheet.

Click here to Download Table S1